ISBN: 978-3-95450-225-7 ISSN: 2673-5571 doi:10.18429/JACoW-HB2021-MOP06

RESONANCE COMPENSATION FOR HIGH INTENSITY AND HIGH BRIGHTNESS BEAMS IN THE CERN PSB

F. Asvesta*, S. Albright, F. Antoniou, H. Bartosik, C. Bracco, G. P. Di Giovanni,
E. H. Maclean, B. Mikulec, T. Prebibaj[1], E. Renner[2]
CERN, Geneva, Switzerland
[1]also at Goethe University, Frankfurt, Germany, [2]also at TU Wien, Vienna, Austria

Abstract

Resonance studies have been conducted during the recommissioning of the CERN Proton Synchrotron Booster (PSB) following the implementation of the LHC Injectors Upgrade (LIU) project. In particular, resonance identification through so-called loss maps has been applied on all four rings of the PSB, revealing various resonances up to fourth order. In a second step, compensation schemes for the observed resonances were developed using a combination of analytical methods, experimental data and machine learning tools. These resonance compensation schemes have been deployed in operation to minimize losses for reaching high intensity and high brightness, thereby achieving the target brightness for the LHC-type beams.

INTRODUCTION

After the completion of the LIU project [1], the PSB faces the challenge of achieving the target values of twice the brightness for the LHC-type beams and increased intensity for the fixed target beams of the various physics users, such as ISOLDE [2] and n-TOF [3], as well as possible future users in the scope of the Physics Beyond Coliders (PBC) project [4]. The main limitations for reaching these goals come from space charge effects, which have been mitigated with the increase in injection energy achieved with the new linear accelerator, Linac4 [5], and the H^- charge exchange injection scheme [6, 7]. However, the β-beating introduced by the injection chicane in the first few ms [8] of the cycle, as well as betatron resonances excited by machine imperfections, still require careful correction for reaching the target beam parameters.

Extended resonance studies were conducted in the pre-LIU era to characterize the resonances, in all PSB rings, at the new injection energy of 160 MeV [9, 10]. The studies, which were used as a preparatory stage for a smoother recommissioning period, revealed several 3rd order normal and skew resonances. It should be noted that the four superposed rings did not behave the same in terms of resonances. For example, in Ring 4 only the normal sextupole resonance, $Q_x + 2Q_y = 13$, was observed while in Ring 3 all skew and normal 3rd order resonances resulted in losses. In addition, the compensation values for the same resonance in different rings, such as the half integer resonance excited in all rings, were different. However, the energy upgrade was only part of the LIU project. The newly installed elements, like the ones needed for the new injection scheme, can have an impact on the excitation of the resonances and hence past studies can only offer an indication of the post-upgrade behaviour. Furthermore, the expected incoherent space charge tune spread at the PSB injection can be, in absolute value, larger than $|\Delta Q_{x,y}| > 0.5$ for the higher brightness beams [11,12]. Consequently, the tunes are set to high values at injection, for example $Q_x = 4.4$ / $Q_y = 4.45$ for these beams. The tunes are then varied during acceleration to reach the optimized extraction tunes of $Q_x = 4.17$ / $Q_y = 4.23$. Hence, the tune space of interest is large and multiple resonances are crossed during normal operation as shown in Fig. 1. In this respect, complete studies in order to identify and compensate any observed resonances were crucial during the commissioning phase to prepare the operational beams.

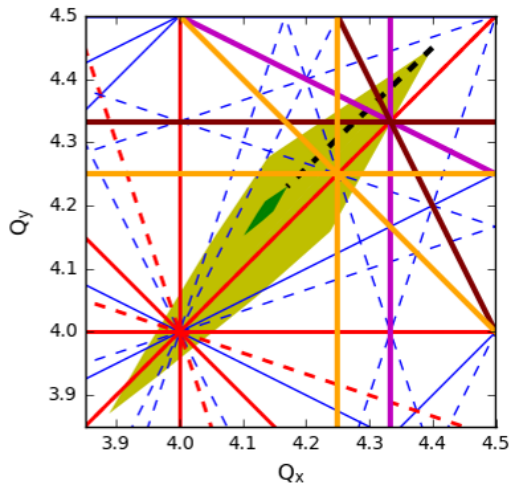

Figure 1: Schematic of the expected incoherent tune spreads at the PSB injection (yellow area) and extraction (green area) for the LHC-type beams. The tunes are varied during the cycle following the dotted black line. Resonance lines up to 4th order are plotted, normal in solid and skew in dashed. The non-systematic resonance lines are plotted in blue and the systematic in red. Potentially excited resonances of interest are highlighted in different colors depending on their order, 3rd order normal in purple, skew in brown and 4th order normal in orange.

RESONANCE IDENTIFICATION

The resonance studies were one of the priorities of the commissioning period in the PSB, as multiple 2nd and 3rd

* foteini.asvesta@cern.ch

ISBN: 978-3-95450-225-7 ISSN: 2673-5571 doi:10.18429/JACoW-HB2021-MOP06

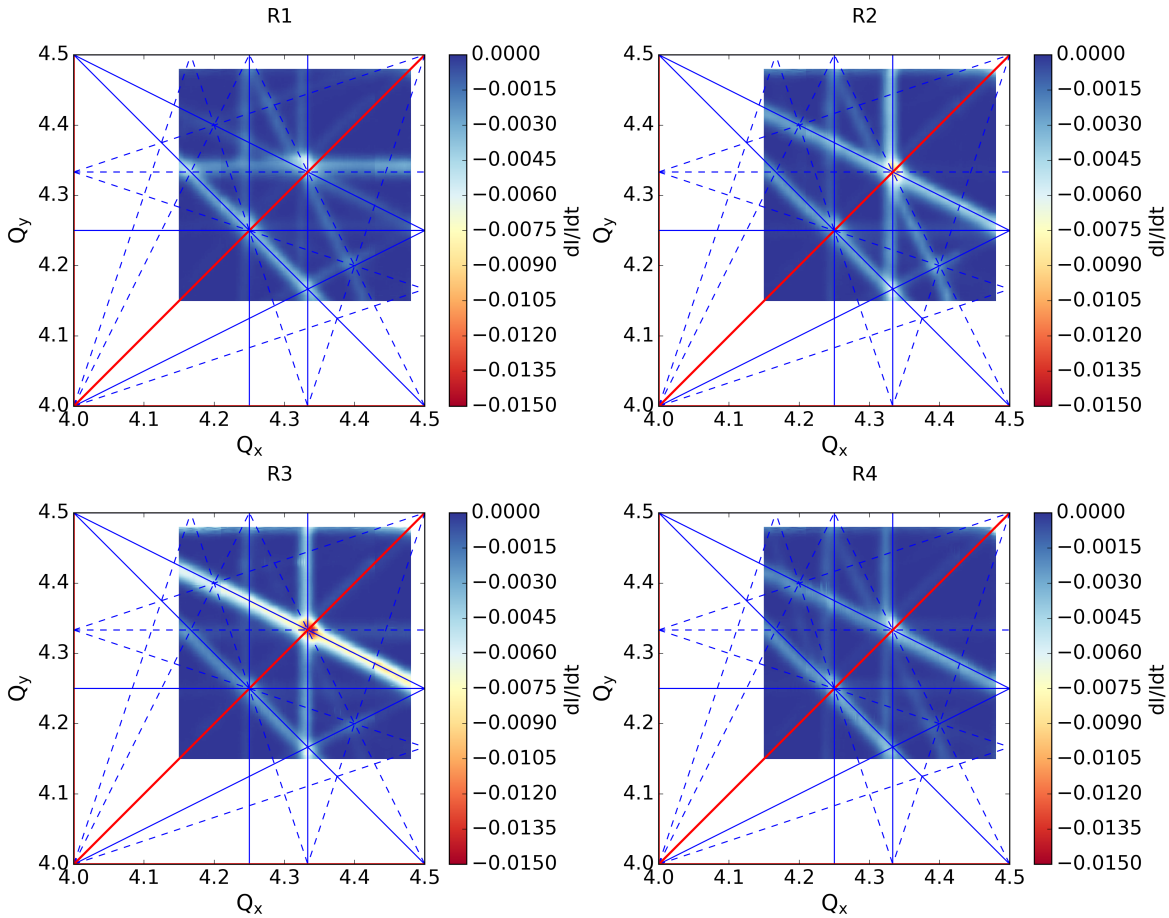

Figure 2: Loss maps resulting from dynamic tune scans in all four rings of the PSB. The transverse tune space is color coded using the loss rate variation. Resonance lines up to 4th order are plotted, normal in solid lines and skew in dashed. The non-systematic resonance lines are plotted in blue and the systematic, the coupling resonance in this case, in red.

order resonances were expected to be excited [10]. In order to identify the resonances in the transverse tune space, the dynamic tune scan technique was used to produce the loss maps. In this technique, one of the tunes is kept constant throughout the cycle while the other one is changed dynamically. At the same time, the intensity is recorded and the resonances are revealed through the induced losses. The range of tunes for the scan is 4.15 to 4.48 and the step for the static tune is 0.0085. For the studies, a flat cycle at the injection energy of 160 MeV is used. In this manner, the beam is stored for a long time, 275 ms to 700 ms, and all resonances are studied at the same energy. It should be highlighted that only cycle times after 350 ms are considered to avoid effects coming from the injection process and ensure that the beam parameters are the same at the beginning of each scan. The beam is setup in order to have a small space charge tune spread of $\Delta Q_{x,y} = -0.035$, as low brightness beams are the most sensitive in terms of losses to machine driven errors [13].

The dynamic tune scans are conducted in all rings of the PSB and in all directions, i.e. four different scans for each ring. Initially the Q_x is kept constant while Q_y varies from max to min following a scan in which it varies from min to max, the same is repeated keeping Q_y constant and varying the Q_x. The different scans are needed as the dynamic tune or the direction of the crossing can have an impact on the observable, i.e. the loss rate. For example, 1D resonances, such as the $3Q_x = 13$, can be completely transparent if they are not dynamically crossed, i.e. varying the Q_x in this case, as on the resonance they create constant losses and not a variation of the loss rate. The direction of the tune sweep can also affect which resonances appears stronger, since the beam degrades during the first crossing of a resonance and subsequent resonance crossings can exhibit a different behavior in terms of loss rate. In the loss maps shown in this paper, the average value for all four scans in each ring is considered.

The resulting loss maps for each ring with the natural excitation of the resonances in the PSB, are shown in Fig. 2. In all rings we can identify resonances up to 4th order. In fact, even though the strength of the resonances is not the same in all rings, as deduced from the presented loss rate, all 3rd (normal and skew) and 4th (normal) order resonances are excited in all rings. It should be noted that this was an unexpected result as the 4th order resonances were not observed in the PSB before the LIU upgrade. In addition,

ISBN: 978-3-95450-225-7 ISSN: 2673-5571 doi:10.18429/JACoW-HB2021-MOP06

previous studies had shown that different resonances were excited in different rings. In the recent results, the only ring that exhibits a different behaviour is Ring 1 as the dominating errors seem to be the ones exciting the 3rd order skew resonances, $3Q_y = 13$ and $2Q_x + Q_y = 13$, and not the 3rd order normal ones, $3Q_x = 13$ and $Q_x + 2Q_y = 13$, as in the other rings. The strongest resonance in terms of losses is the $Q_x + 2Q_y = 13$ in Ring 3. This resonance is observed inducing less losses in the other rings. Finally, the half integer resonance was not included in the scan as the full beam is lost once the 4.5 tune is approached in either plane.

RESONANCE COMPENSATION

The naturally excited 2nd and 3rd order resonances in the PSB can be compensated using the available correctors as demonstrated in the past [10, 14]. Even though 4th order resonances had not been previously observed, the PSB is equipped with octupole correctors that could act on the observed resonances. To compensate the resonances, a technique based on both analytical tools (Resonance Driving Terms (RDT) analysis using PTC [15] in MADX [16]) and experimental data (intensity monitoring while dynamically crossing the resonance and varying the corrector strengths) is used, as described in [10, 13, 17].

Vertical Half Integer Resonance

The resonance at $Q_y = 4.5$ is the strongest in the regime of interest for the operation of the PSB. The injection working point for the high brightness beams is $Q_x = 4.40$ / $Q_y = 4.45$ as shown in Fig. 1. Past studies had suggested pushing it above the half integer resonance at $Q_x = 4.43$ / $Q_y = 4.60$ to improve brightness [9]. As a result, the first compensation studies focused on the $2Q_y = 9$ resonance. In the past, the half integer resonance was perfectly compensated [10]. Currently only a partial compensation is possible with $\approx 5\%$ remnant losses during the crossing as seen in Fig. 3 where the natural excitation and the best found configuration are given. It should be noted that this is not correlated to the β-beating induced by the injection chicane, as the resonance is studied long after the injection process has finished. The fact that the half integer is not perfectly compensated is a limitation for the brightness and the high intensity beams for tunes $Q_y > 4.5$. Consequently, all operational beams are currently setup below the $2Q_y = 9$.

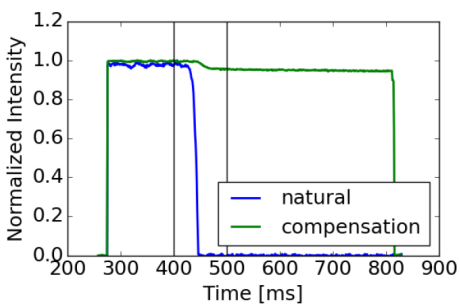

Figure 3: Normalized intensity while crossing the half integer resonance from 400 ms to 500 ms with the natural excitation (blue) and after the compensation (green).

High Order Resonances

Nonlinear higher order resonances are compensated following the same procedure. For each resonance the corresponding correction magnets are used, i.e. sextupoles are used for 3rd order normal, skew sextupoles for 3rd order skew and octupoles for 4th order normal resonances. Every time two correctors (orthogonal for the corresponding RDT) are varied and only one resonance is crossed. Like this, the magnet strengths can be used in the MADX PSB model to identify the RDT of the excitation and characterize the resonance.

Resonances of 3rd order, both normal and skew, are always fully compensated, however, the 4th order resonances could only be partially corrected. Figure 4 shows two representative cases, one of a full compensation of a 3rd order normal resonance (left) and one of a partial compensation of a 4th order resonance (right). The resonance is fully compensated as a region with practically no losses is identified in Fig. 4 (left). On the other hand, the compensation of the 4th resonance cannot be further improved as the correctors are running out of their limits (±50 A) before the losses are completely eliminated in Fig. 4 (right). It is worth noting that in the half integer case discussed previously the limitation for the compensation is not coming from the current as the minimum loss region was fully identified.

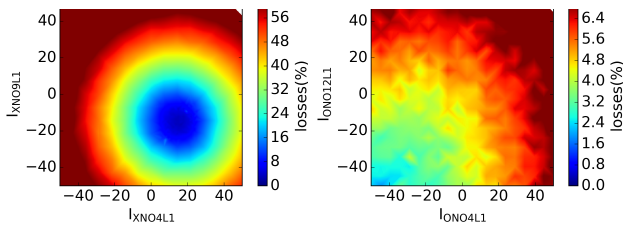

Figure 4: Current configuration of the corresponding correctors to compensate a normal sextupole (left) and normal octupole (right) resonance color coded to the measured losses as the resonance is being crossed.

Given the fact that during normal operation the tune in the PSB changes, as shown in Fig. 1, it is important to investigate global corrector settings that can compensate all resonances of concern at the same time. In this manner, no losses or emittance blow-up should be induced when the resonances are crossed or overlapped due to the space charge induced tune shift. Global settings for the 4th order resonances were found experimentally, as all resonances had similar compensation values. It is reminded that, as shown in Fig 4, the compensation for the octupoles is partial. However, for the 3rd order resonances, the settings of the correctors were different for each resonance and no global corrections could be found experimentally.

Using in the MADX model the corrector settings found experimentally, the RDT of the error that drives each resonance can be approximated. Calculating the RDTs of each

ISBN: 978-3-95450-225-7 ISSN: 2673-5571 doi:10.18429/JACoW-HB2021-MOP06

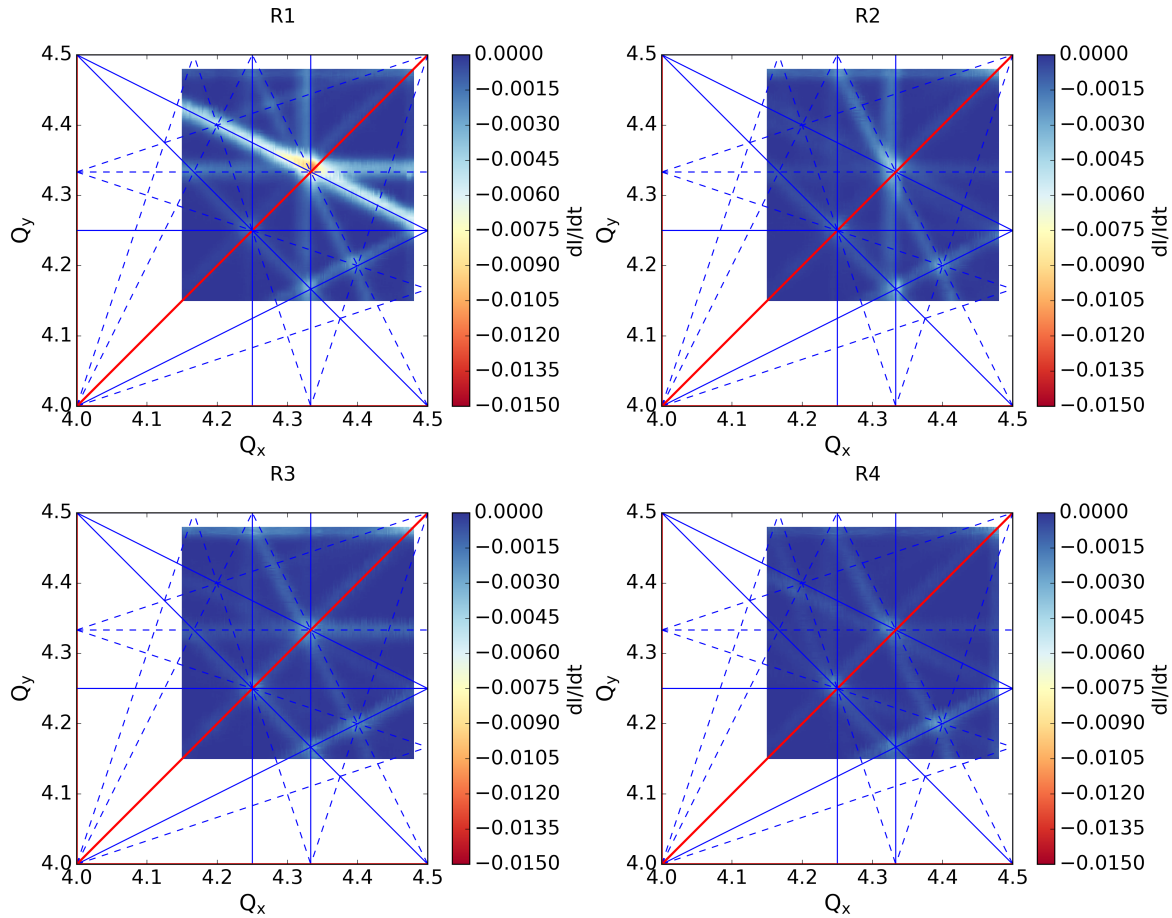

Figure 5: Loss maps resulting from dynamic tune scans in all four rings of the PSB with octupoles and sextupoles for the simultaneous correction of the 3rd and 4th order normal resonances. Note that in R2 only one of the 3rd order normal resonances is compensated. The transverse tune space is color coded using the loss rate variation. Resonance lines up to 4th order are plotted as in Fig. 2.

available corrector magnet on the crossing point of the resonances, one could try and characterize the combined effect of each magnet to all considered resonances. For example, performing the RDT analysis at $Q_{x,y} = 4.33$, i.e. the crossing point for two 3rd order normal resonances $3Q_x = 13$ and $Q_x + 2Q_y = 13$, this response matrix can be devised:

$$\begin{bmatrix} Re[RDT^{sext1}_{3Qx}] & Re[RDT^{sext2}_{3Qx}] & Re[RDT^{sext3]}_{3Qx} & Re[RDT^{sext4}_{3Qx}] \\ Im[RDT^{sext1}_{3Qx}] & Im[RDT^{sext2}_{3Qx}] & Im[RDT^{sext3}_{3Qx}] & Im[RDT^{sext4}_{3Qx}] \\ Re[RDT^{sext1]}_{Qx+2Qy} & Re[RDT^{sext2}_{Qx+2Qy}] & Re[RDT^{sext3}_{Qx+2Qy}] & Re[RDT^{sext4}_{Qx+2Qy}] \\ Im[RDT^{sext1}_{Qx+2Qy}] & Im[RDT^{sext2}_{Qx+2Qy}] & Im[RDT^{sext3}_{Qx+2Qy}] & Im[RDT^{sext4}_{Qx+2Qy}] \end{bmatrix} \times \begin{bmatrix} F_{k^{sext1}} \\ F_{k^{sext2}} \\ F_{k^{sext3}} \\ F_{k^{sext4}} \end{bmatrix} = \begin{bmatrix} Re[RDT^{meas}_{3Qx}] \\ Im[RDT^{meas}_{3Qx}] \\ Re[RDT^{meas}_{Qx+2Qy}] \\ Im[RDT^{meas}_{Qx+2Qy}] \end{bmatrix} \quad (1)$$

where, the real and imaginary parts of the measured RDTs and the RDTs from the individual sextupoles can be used to identify the factors $F_{k^{sext(1,2,3,4)}}$ that are needed in all sextupoles to compensate both resonances at the same time. Note that in order to acquire a global solution using this technique, at least two correctors are needed for each resonance, i.e. 4 in this example. Due to current limitations, the solution for ring 2 could not be used and in ring 1 an extra sextupole magnet, i.e. 5 in total, had to be included. To add this extra magnet, the combined RDT of two sextupoles powered at the same current was used in Eq. (1). This procedure was followed for the 3rd order normal resonance but could not be tested for the skew resonances, as only three skew sextupole correctors are currently connected in all rings.

The global settings for the octupoles and the normal sextupoles are tested experimentally in the machine and the resonance identification studies are repeated. The resulting loss maps with the settings for the compensation of 3rd and 4th order normal resonances are given in Fig. 5. The 4th order resonances seem to be corrected at a satisfactory

ISBN: 978-3-95450-225-7 ISSN: 2673-5571 doi:10.18429/JACoW-HB2021-MOP06

level in all rings. On the other hand, the sextupole resonances appear well compensated in rings 2, 3 and 4 (recall that in ring 2 only the setting for the $Q_x + 2Q_y = 13$ is active), but in ring 1 the situation is quite different. The normal sextupole resonances, which were not very strong naturally as shown in Fig. 2, appear substantially enhanced. This implies a cross talk between the corrector magnets and resonances, other than the ones they are compensating. To investigate this interaction further loss maps compensating the sextupole and octupole resonances alone were performed and are shown in Figs. 6 and 7 respectively. Figure 6 shows that the analytically acquired global compensation values for the sextupole resonances in rings 1, 3 and 4 work as expected and do not affect the other resonances. In the case of octupoles however, (Fig. 7), while the 4th order resonances are compensated the 3rd order resonances, especially the normal ones, are strongly enhanced in all rings.

Optimizer Tools

The significant cross talk of the correctors with the resonances and the difficulties in identifying global settings for the skew sextupoles pushed for further optimizations of the compensation schemes. To this end, the tool Generic Optimisation Frontend and Framework (GeOFF) [18], which uses the python implementation of the algorithm for bound constrained optimization without derivatives, pyBOBYQA [19–21], was used to refine the scheme.

The optimization tool significantly reduces the time needed for the corrector current scans as it diminishes the need for a full scan of the parameter space. Consequently, it's possible to use more corrector magnets to improve the compensation of partial corrected resonances as well as investigate global settings experimentally. As a first step, the resonances were tackled individually. The compensation settings for several resonances appeared different than what was measured at the beginning of the year. It should be noted that these differences are not connected to the new tools used but rather indicate that since the commissioning the errors changed. Furthermore, the 4th order compensation was improved using all the available octupoles (four per ring) and global settings for the 3rd order skew resonances were found using all skew sextupoles (three per ring). These optimized settings have improved the performance of the machine, contributing to the increased brightness [8]. However, studies are still ongoing to further characterize the resonances and improve the performance exploiting the full potential of the optimizer framework.

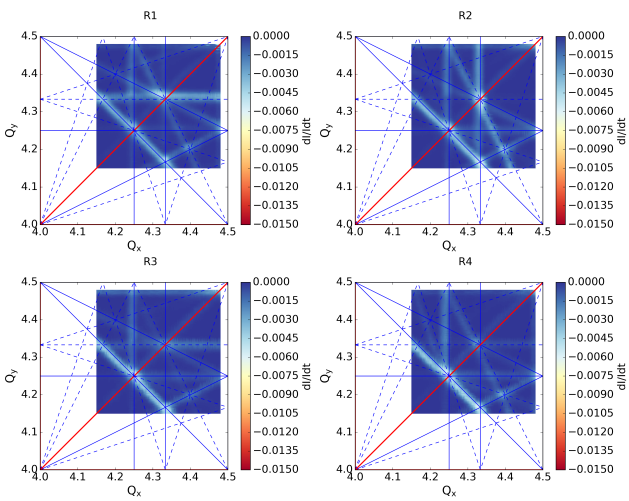

Figure 6: Loss maps resulting from dynamic tune scans in all four rings of the PSB with sextupoles for the compensation of the 3rd order normal resonances, $3Q_x = 13$ and $Q_x + 2Q_y = 13$. Note that in R2 only the $Q_x + 2Q_y = 13$ is compensated as not enough correctors were available. The transverse tune space is color coded using the loss rate variation. Resonance lines up to 4th order are plotted as in Fig. 2.

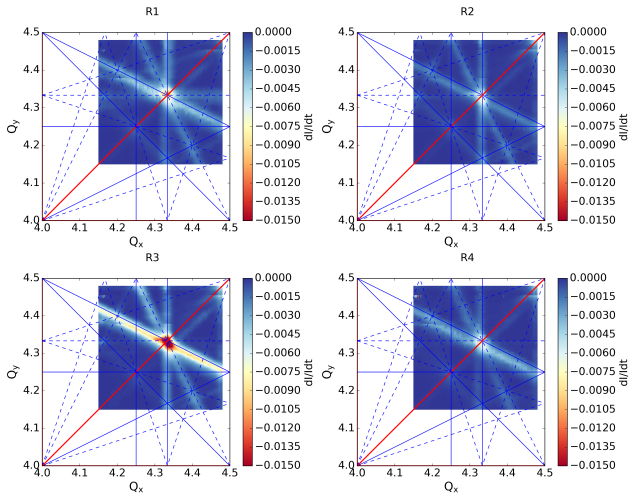

Figure 7: Loss maps resulting from dynamic tune scans in all four rings of the PSB with octupoles for the compensation of the 4th order normal resonances, $4Q_x = 17$, $4Q_y = 17$ and $2Q_x + 2Q_y = 17$. The transverse tune space is color coded using the loss rate variation. Resonance lines up to 4th order are plotted as in Fig. 2.

CONCLUSION

Resonance studies were conducted in the PSB during the commissioning period after the upgrade in the frame of the LIU project. The studies revealed resonances up to 4th order in all rings, that were observed for the first time. Compensation schemes allowing for global compensation of the resonances were developed through extensive experimental and analytical studies. Refinement of the schemes with optimizer tools provides a better compensation for all resonances and has contributed to higher brightness and intensity for the PSB users.

ACKNOWLEDGEMENTS

The authors would like to thank the PSB Operations and commissioning teams for their support during the experiments and A. Huschauer, V. Kain and N. Madysa for the optimization tools used during the resonance compensation campaign.

ISBN: 978-3-95450-225-7 ISSN: 2673-5571 doi:10.18429/JACoW-HB2021-MOP06

REFERENCES

[1] H. Damerau *et al.*, "LHC Injectors Upgrade, Technical Design Report, Vol. I: Protons", Technical Report, CERN-ACC-2014-0337, Dec 2014.

[2] B. Jonson and K. Riisager, "The ISOLDE facility", *Scholarpedia*, vol. 5, no. 7, p. 9742, 2010. doi:10.4249/scholarpedia.9742

[3] A. Mengoni *et al.*, "Status and perspectives of the neutron time-of-flight facility nTOF at CERN", *EPJ Web Conf.*, vol. 239, p. 17001, 2020. doi:10.1051/epjconf/202023917001

[4] J. Jaeckel, M. Lamont, and C. Vallee "The quest for new physics with the Physics Beyond Colliders programme", *Nat. Phys.*, vol. 16, pp. 393–401. 2020. doi:10.1038/s41567-020-0838-4

[5] L. Arnaudon *et al.* "Linac4 Technical Design Report", CERN, Geneva, Switzerland, Rep. CERN-AB-2006-084, 2006

[6] E. Renner *et al.*, "Beam Commissioning of the New 160 MeV H- Injection System of the CERN PS Booster", in *Proc. 12th Int. Particle Accelerator Conf. (IPAC'21)*, Campinas, Brazil, May 2021, paper WEPAB210, pp. 3116–3119. doi:10.18429/JACoW-IPAC2021-WEPAB210

[7] E. H. Maclean *et al.*, "Optics Measurement by Excitation of Betatron Oscillations in the CERN PSB", in *Proc. 12th Int. Particle Accelerator Conf. (IPAC'21)*, Campinas, Brazil, May 2021, pp. 4078–4081. doi:10.18429/JACoW-IPAC2021-THPAB168

[8] T. Prebibaj *et al.*, "Injection chicane beta-beating correction for enhancing the brightness of the CERN PSB beams", presented at HB'2021, Fermilab, Batavia, IL, USA, Oct. 2021, paper MOP18, this conference.

[9] V. Forte, "Performance of the CERN PSB at 160 MeV with H^- charge exchange injection", 2016. https://cds.cern.ch/record/2194937

[10] A. Santamaria Garcia *et al.*, "Identification and Compensation of Betatronic Resonances in the Proton Synchrotron Booster at 160 Mev", in *Proc. 10th Int. Particle Accelerator Conf. (IPAC'19)*, Melbourne, Australia, May 2019, pp. 1054–1057. doi:10.18429/JACoW-IPAC2019-MOPTS086

[11] B. Mikulec, A. Findlay, V. Raginel, G. Rumolo, and G. Sterbini, "Tune Spread Studies at Injection Energies for the CERN Proton Synchrotron Booster", in *Proc. HB2012*, Beijing, China, Sept. 2012, paper MOP249, pp. 175–179.

[12] E. Benedetto *et al.*, "CERN PS Booster Upgrade and LHC Beams Emittance", in *Proc. 6th Int. Particle Accelerator Conf. (IPAC'15)*, Richmond, VA, USA, May 2015, pp. 3897–3900. doi:10.18429/JACoW-IPAC2015-THPF088

[13] F. Asvesta, H. Bartosik, S. Gilardoni, A. Huschauer, S. Machida, Y. Papaphilippou, and R. Wasef, "Identification and characterization of high order incoherent space charge driven structure resonances in the CERN Proton Synchrotron", in *Phys. Rev. Accel. Beams*, vol. 23, no. 9, 2020, doi:10.1103/PhysRevAccelBeams.23.091001

[14] P. Urschütz, "Measurement and Compensation of Second and Third Order Resonances at the CERN PS Booster", in *Proc. 9th European Particle Accelerator Conf. (EPAC'04)*, Lucerne, Switzerland, Jul. 2004, paper WEPLT03, pp. 1918-1920.

[15] F. Schmidt, E. Forest, and E. McIntosh, "Introduction to the polymorphic tracking code: Fibre bundles, polymorphic Taylor types and 'Exact tracking'", CERN-Report *CERN-SL-2002-044-AP. KEK-REPORT-2002-3*, 2002.

[16] L. Deniau, E. Forest, H. Grote, and F. Schmidt, computer code MAD-X, 2016. http://madx.web.cern.ch/madx/

[17] F. Asvesta, H. Bartosik, A. Huschauer, Y. Papaphilippou, and G. Sterbini, "Resonance Identification Studies at the CERN PS", in *Proc. 9th Int. Particle Accelerator Conf. (IPAC'18)*, Vancouver, Canada, Apr.-May 2018, pp. 3350–3353. doi:10.18429/JACoW-IPAC2018-THPAK056

[18] V. Kain and N. Madysa, "Generic Optimisation Frontend and Framework (GeOFF)". https://gitlab.cern.ch/vkain/acc-app-optimisation

[19] M. Powell, "The BOBYQA Algorithm for Bound Constrained Optimization without Derivatives." *Technical Report*, Department of Applied Mathematics and Theoretical Physics, 2009.

[20] C. Cartis, J. Fiala, B. Marteau, and L. Roberts, "Improving the Flexibility and Robustness of Model-Based Derivative-Free Optimization Solvers", *ACM Transactions on Mathematical Software*, 45:3 (2019), pp. 32:1-32:41. arXiv:1804.00154

[21] C. Cartis, L. Roberts, and O. Sheridan-Methven, "Escaping local minima with derivative-free methods: a numerical investigation, Optimization" (2021). arXiv:1812.11343